Vol 15 No 11, November 2006
1009-1963/2006/15(11)/2558-06
Chinese Physics
© 2006 Chin. Phys. Soc.
and IOP Publishing Ltd

Influence of the probe–sample interaction on scanning near-field optical microscopic images in the far field*

Li Zhi(李 智), Zhang Jia-Sen(张家森)†,
Yang Jing(杨 景), and Gong Qi-Huang(龚旗煌)‡

Department of Physics and State Key Laboratory for Mesoscopic Physics, Peking University, Beijing 100871, *China*

(Received 30 March 2006; revised manuscript received 18 April 2006)

We have studied the influence of probe–sample interaction in a scanning near-field optical microscopy (SNOM) in the far field by using samples with a step structure. For a sample with a step height of $\sim \lambda/4$, the SNOM image contrast between the two sides of the step changes periodically at different scan heights. For a step height of $\sim \lambda/2$, the image contrast remains approximately the same. The probe–sample interaction determines the SNOM image contrast here. The influence of different refractive indices of the sample has been also analysed by using a simple theoretical model.

Keywords: SNOM, probe–sample interaction, near-field scanning optical microscopy
PACC: 0779, 6116P

1. Introduction

The optical resolution in traditional far-field optics can only reach $\sim \lambda/2$, since it is limited by the Rayleigh diffraction. By the use of evanescent waves, a scanning near-field optical microscope (SNOM)[1−3] can break this limit. In most common cases, the aperture SNOM uses a tapered metal-coated optical fibre[4,5] whose aperture diameter is about a few tens of nanometres. The light emitted from the fibre probe illuminates the sample surface in the near-field region. Either the reflected or the transmitted signal is detected in the far field, which gives the optical contrast. This is called the illumination mode (I-mode). In a collection mode (C-mode) SNOM,[6,7] the sample is illuminated as in a conventional microscope with an extended beam, and the nanometric fibre tip is used to probe the scattered optical field distribution in the near field. This makes the SNOM a key imaging tool for the local characterization of optical fields in nanoscale photonic structures.[8−11] The C-mode SNOM can also probe the field distribution in the far field.[12] Thus together with the corresponding results in the near field, it can give a complete picture of the complex light field evolution process from near field to far field.

To interpret the SNOM image, one must pay attention to the sample topography[13] and the probe–sample interaction because they mix with the true optical field and make the signal complicated. In the constant-height mode (CHM) operation, topography artifacts can be removed[13] and the probe–sample interaction will be the main source for the complexity. Campillo *et al*[14] showed that due to the probe–sample interaction in photonic structures made from arrays of air holes in a Si_3N_x membrane, the holes appeared dark and the film was bright in the transmission SNOM counterintuitively.

In this paper, we study the influence of the probe–sample interaction in a transmission SNOM working in the far field region. Using a step structure, we show how the probe–sample interaction changes the image contrast between the two sides of the step at different scan heights. Then the influence of different step heights is discussed. Finally we give a theoretical discussion on the effect of different refractive indices of the sample.

*Project supported by the National Natural Science Foundation of China (Grant Nos 90206003, 10374005, 10434020, 10521002, 10328407 and 90101027) and the Research Fund for the Doctoral Program of Higher Education of China (Grant No 20040001012).
†E-mail: jszhang@pku.edu.cn
‡E-mail: qhgong@pku.edu.cn

2. Experiment and results

In the experiment, we used an Omicron Twin SNOM in a transmission mode, as schematically shown in Fig.1. A laser light at $\lambda = 635$nm with a power of about 1mW was coupled into the fibre. Then the Al-coated fibre tip, whose optical aperture was about 50 nm, illuminated the sample surface. A 100× immersion oil objective with NA=1.25 was used to collect the transmitted light. Then after passing through a diaphragm, the collected light was focused on a photo-multiplier (PMT). The diameter of the diaphragm could be adjusted from 1 to 7 mm to change the detected signal. Since we focused on the far-field effect of the probe–sample interaction here, CHM scanning mode was mainly used to scan the probe at a constant height of a few tens to hundreds of nanometres over the sample. We also measured the sample topography by the constant-gap mode (CGM) and the shear-force feedback system was used to keep the tip–sample distance at a few nanometres.

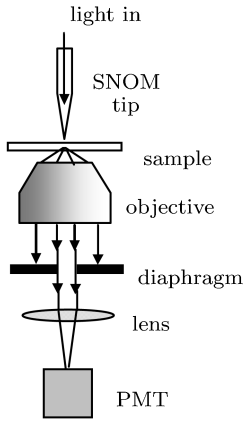


Fig.1. Schematic of the experimental setup.

According to Helmholtz' reciprocity theorem,[15] the I-mode and the C-mode SNOM are equivalent in principle. In experiments, the I-mode is usually used to provide a better signal to noise ratio due to the smaller excitation area and less stray light, as we did here. The analyses in our work were done from the view of C-mode to give a more intuitive physical image, however the conclusions are appropriate for both modes. In the experiment, we set the diaphragm to the smallest diameter. As a result, only light near the optical axis could be detected (see Fig.1). From the view of the C-mode, this case corresponds to illuminating the sample normally by a nearly parallel light, which is usually the interested situation. For a flat homogeneous sample, nearly parallel light illumination should induce an approximate homogeneous optical field over it. Figure 2(a) shows the measured approach curve, which is the optical signal I as a function of the probe/sample distance z. It was taken on a flat cover slip. Unlike our expectation, the measured approach curve shows an evident oscillating behaviour. This is because when the probe is present, light is reflected between the probe and the sample. As a consequence the reflected light coherently superimposes upon the incident light, resulting in an oscillating signal. Its oscillation period should be $\sim \lambda/2$, which can be seen in Fig.2(a). When the fibre probe detects the optical field, the probe–sample interaction changes the optical field and gives an additional component to the SNOM signal. From the approach curve, we can see that this component depends on the probe/sample distance z and cannot be ignored even in the far field. It may greatly affect the far-field SNOM image.

To illustrate this effect, let us refer to Fig.2(b) which shows a step-structure sample consisting of the same optical material. If the step height is much smaller than the whole sample thickness, the approach curves on the two flat sides of the step should be nearly the same (see the approach curves in Fig.2(b)) except for the transition region quite near the step. For a CHM scan at a height of h over the step, its detected signal on the left side of the step corresponds to a probe/sample distance of $z = h$ in the approach curve, while on the right side the probe/sample distance should be $z = h + d$, where d is the step height. For a step height of about $\lambda/4$, it means when one side of the step is at the oscillation peak of the approach curve, the other side is just at the valley. As the scan height h changes, the signal contrast between the two sides then changes periodically. If the step height is just about $\lambda/2$, signals on the two sides reach the valleys or peaks at the same time, so that the resulting CHM contrast remains the same as h changes.

To demonstrate the effect experimentally, we spin-coated a poly (methyl methacrylate) (PMMA) film on a cover slip first. Then a groove was made on it by mechanical scratching and the step structure was formed at the edge of the groove. Figure 2(c) displays the experimental topography profile of one of the samples obtained in a CGM SNOM by the shear-force control mechanism. The step height is a few hundreds of nanometres, which is much smaller than the thickness of the cover slip base. We used PMMA in the

experiment because its refractive index is about 1.49 at λ=635nm, which is quite close to the refractive index of the cover slip, 1.51. The reflection between the film and the cover slip is negligible and we can consider them as the same optical material approximately. The measured approach curve on the film is the same as on the cover slip base within experimental errors, which also indicates that the approximation is reasonable. By changing the concentration of the PMMA solution we can change the step height. In the experiment, we chose the step heights to be 165 and 330nm, namely $\sim \lambda/4$ and $\sim \lambda/2$, respectively.

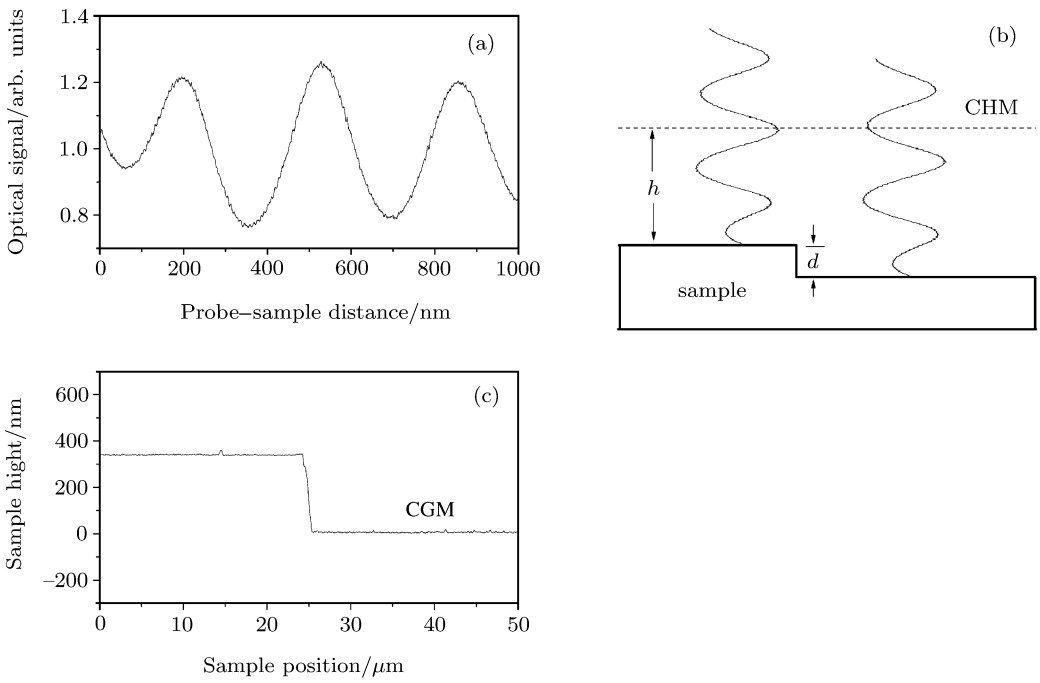


Fig.2. (a) Approach curve measured on the cover slip. (b) Schematic of the influence of the probe–sample interaction on the CHM scan signals. (c) Topography profile of one of the samples obtained in the CGM SNOM by the shear-force technique.

For a step height of d=165nm, the resulting CHM signals are shown in Figs.3(a)–3(e) for h=60, 190, 360, 520, and 690nm, respectively. Here, we focus on the signals over the two sides of the step and ignore the complex optical structures in the transition region due to diffraction and other effects. For each side, we can find the corresponding positions in the approach curve for Figs.3(a)–3(e), respectively. They are indicated by arrows in Fig.3(f), where the symbols a–e mean the corresponding CHM images, and L and R represent the left and right sides of the step respectively. We can see that, for Figs.3(a), 3(c), and 3(e), signals on the left side of the step correspond to the oscillation valleys in the approach curve, indicating that the probe–sample interaction gives negative additional signals, and thus smaller total signals. At the same time, signals on the right side correspond to the peaks, and this results in positive additional signals, and thus larger total signals. The opposite situations appear in Figs.3(b) and 3(d). Thus, as predicted, the contrast reversal behaviour is quite obvious in Figs.3(a)–3(e) as h changes. Comparisons between the CHM signals and the signals in the corresponding approach curve show that they coincide very well.

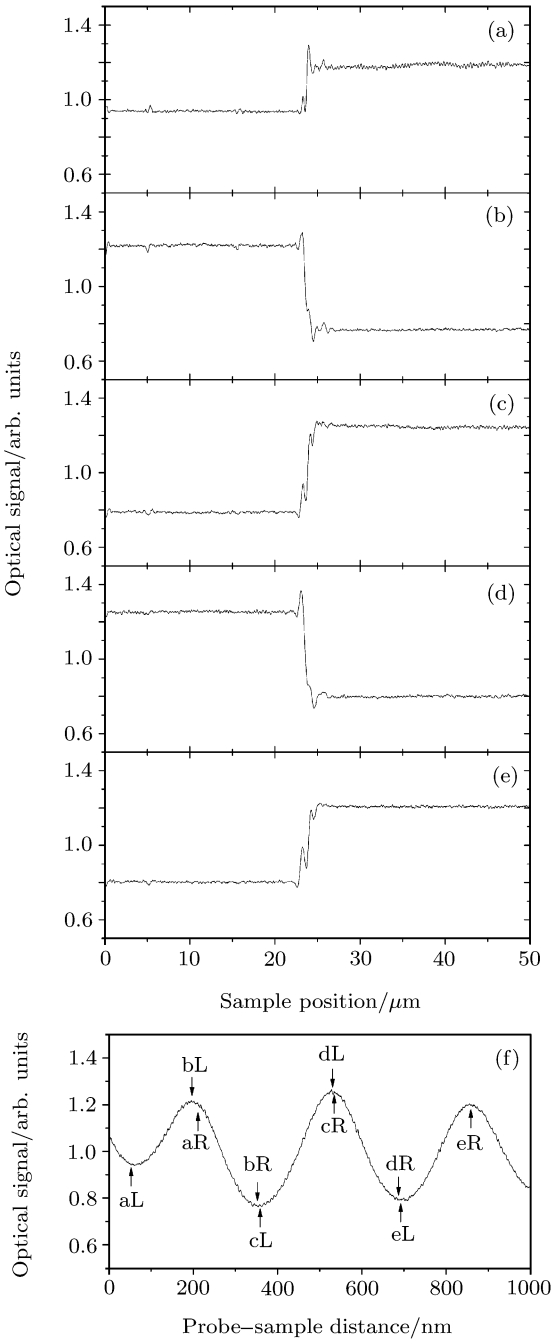


Fig.3. (a)–(e), the CHM scan signals for the scan heights h=60, 190, 360, 520, and 690nm, respectively, with the step height d=165nm. (f) is the corresponding approach curve.

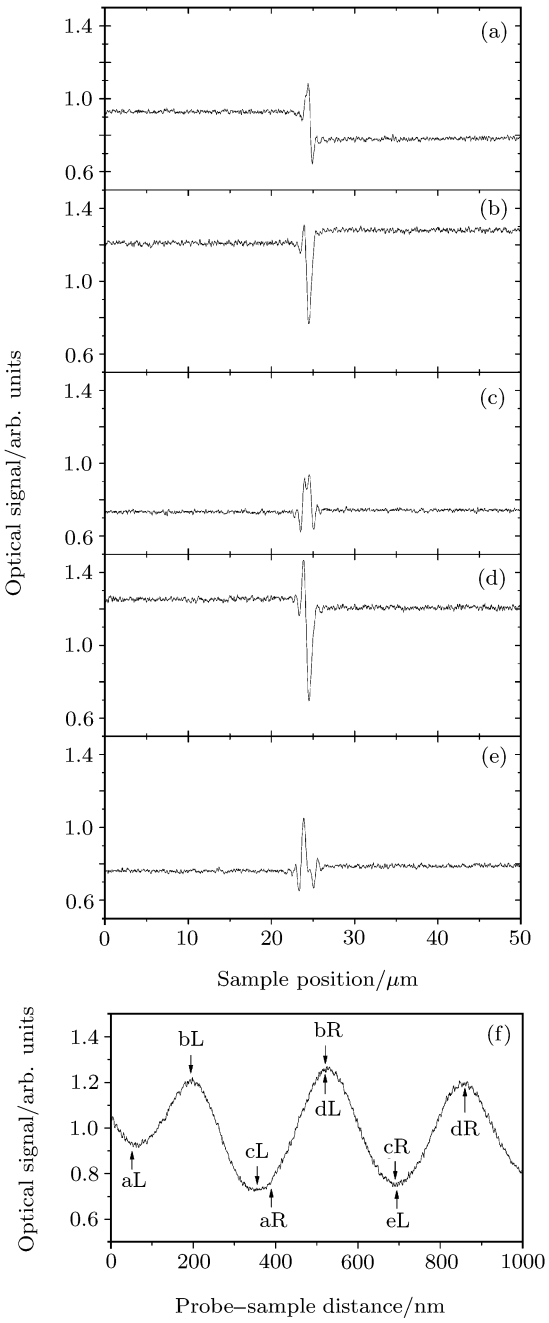


Fig.4. (a)–(e), the CHM scan signals for the scan heights h=60, 190, 360, 520, and 690nm, respectively, with step height of d=330nm. (f) is the corresponding approach curve.

For a step height of d=330nm, Figs.4(a)–4(e) display the CHM signals at h=60, 190, 360, 520, and 690nm, respectively. We also indicate their corresponding positions in their approach curve in Fig.4(f). Here, the signals on the two sides of the step reach the oscillation valleys or peaks at the same time, so that they equal each other approximately in Figs.4(b)–4(e) and the contrast reversal behaviour for the d=165nm case does not occur. In Fig.4(a), the difference between the signals on the two sides is somewhat evident. This comes from the reduced oscillating amplitude of the approach curve at a small probe/sample distance z. A real fibre probe may have a complex tip shape and metal coating. When it is very near to the sample, complex probe–sample interactions and other effects may reduce the coherent behaviour and the resulting oscillating amplitude. Nevertheless, despite all the small discrepancies, we must say that the probe–

sample interaction has a much smaller influence on the image contrast for a step height of $\sim \lambda/2$.

Under nearly parallel light illumination, since the optical field on the two sides of the step should be the same without the probe for any step height, we can say that the probe–sample interaction dominates the SNOM image contrast here. For a step height of an arbitrary value, the effect lies between the $d = \lambda/4$ and $\lambda/2$ cases. The image contrast between the two sides should also change periodically, but is not as distinct as in the $d = \lambda/4$ case.

3. Theoretical discussion

Because of the major role of the approach curve, we give a simplified theoretical discussion on how it is affected by the refractive index of the film. The schematic diagram is shown in Fig.5. We denote the refractive indices of the cover slip base and film as n_1 and n_2. The light coming out of the fibre probe is reflected at the sample surface, the sample/cover slip interface and the probe surface. We use r_1 and t_1 to denote the complex amplitude reflectivity and transmittance for the light from the air into the sample, r_1' and t_1' from the sample into the air, and r_2 and t_2 from the sample into the cover slip, respectively. The effective complex amplitude reflectivity at the probe surface, r, includes the influences due to diffractions and other effects.

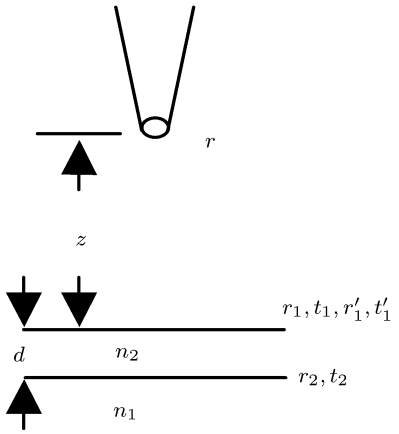


Fig.5. Configuration and the related symbols of the theoretical model.

Here we assume the light to be parallel approximately, which corresponds to an extreme small diaphragm detection condition. For most common materials, their refractive indices n_2 lie between 1.3 and 2.5 and we can treat n_1 as 1.5. Then simple calculations tell us the modules of r_1, r_1' and r_2 are smaller than 0.5. Thus we can ignore multiple reflections here, and the resulting complex amplitude of the detected light should be

$$\begin{aligned} A =& t_1 t_2 \exp(\mathrm{i} n_2 k d)[1 + r_1 r \exp(2\mathrm{i} k z) \\ &+ r_2 r t_1 t_1' \exp(2\mathrm{i} k z + 2\mathrm{i} k n_2 d) \\ &+ r_2 r_1' \exp(2\mathrm{i} k n_2 d)]. \end{aligned} \tag{1}$$

In the first-order approximation, the oscillating component of the detected light intensity is

$$\begin{aligned} I^{\mathrm{osci}} =& 2 t_1^2 t_2^2 |r_1 r| [\cos(2kz) + (r_2 t_1 t_1'/r) \\ &\times \cos(2kz + 2k n_2 d)]. \end{aligned} \tag{2}$$

For the special case of $n_2 = n_1$, this component becomes

$$I^{\mathrm{osci}}_{n_2=n_1} = 2 t^2_{1,n_2=n_1} |r_{1,n_2=n_1} r| \cos(2kz). \tag{3}$$

This means that the approach curve oscillates with a period of $\lambda/2$, and this agrees well with the main feature of the experimental approach curve in Fig.2(a). For $n_2 \neq n_1$, the approach curve also oscillates with a period of $\lambda/2$, but has a different phase and amplitude depending on the sample thickness d. If we define $\eta = r_2 t_1 t_1'/r_1$, we obtain the phase shift and the relative oscillating amplitude, as compared with the $n_2 = n_1$ case,

$$\varphi = \tan^{-1} \frac{\eta \sin(2k n_2 d)}{1 + \eta \cos(2k n_2 d)} \tag{4}$$

and

$$\begin{aligned} \frac{I^{\mathrm{osci}}}{I^{\mathrm{osci}}_{n_2=n_1}} =& \frac{t_1^2 t_2^2 |r_1|}{t^2_{1,n_2=n_1} |r_{1,n_2=n_1}|} \\ &\times [1 + \eta^2 + 2\eta \cos(2k n_2 d)]^{1/2}. \end{aligned} \tag{5}$$

They both change with a period of $\lambda/2n_2$ as the film thickness d changes. For the phase shift, its maximum value is $|\varphi|_{\max} = \tan^{-1}(\eta/\sqrt{1-\eta^2}) = \sin^{-1}|\eta|$. We show how it changes as n_2 varies from 1.3 to 2.5 in Fig.6(a). The resulting maximum phase shift is about 30 degrees. For the relative oscillating amplitude, it varies between $\dfrac{t_1^2 t_2^2 |r_1|}{t^2_{1,n_2=n_1} |r_{1,n_2=n_1}|}(1 - |\eta|)$ and $\dfrac{t_1^2 t_2^2 |r_1|}{t^2_{1,n_2=n_1} |r_{1,n_2=n_1}|}(1 + |\eta|)$. Figure 6(b) shows the dependence of these two values and their average on n_2. Compared with the oscillating amplitude of the $n_2 = n_1$ case, this oscillating amplitude can vary from less than 40% to more than 240% as d and n_2 change. So we can conclude that, for samples with different refractive indices, the probe–sample interaction induces different phases and amplitudes in their corresponding

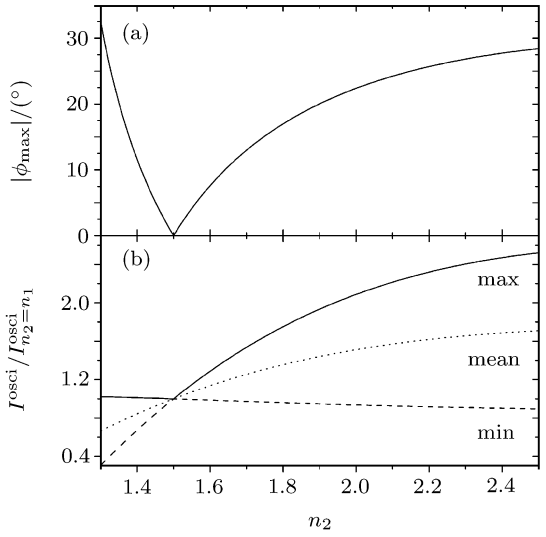


Fig.6. (a) Maximum phase shift of the approach curve compared with the $n_2 = n_1$ case for different n_2. (b) Oscillating amplitude of the approach curve normalized to that of the $n_2 = n_1$ case for different n_2: its minimum, maximum and the mean values.

approach curves, namely different additional signals. Consequently, for a flat sample consisting of different optical materials at different areas, these different additional signals will greatly affect the CHM image. In fact, our step structure can be considered as such a flat sample, for instance, it has a refractive index of 1.5 on one side and a refractive index of 1 on the other side.

4. Conclusion

We have shown that the probe–sample interaction greatly affected the SNOM signals in the far field. The probe–sample interaction gave an additional oscillating component to the SNOM signals depending on the probe/sample distance for a flat homogeneous sample. Then using the step structure with a step height of $\sim \lambda/4$, we have shown how the effect changed the CHM scan image contrast between the two sides of the step at different scan heights. However, for a sample with a step height of $\sim \lambda/2$, little changes was observed. Finally the influence of different refractive indices of the sample on the approach curve was discussed by using a simple theoretical model. To emphasize and clarify the effect of the probe–sample interaction in the far field, we used a large-scale sample in the experiment. For a real sample with smaller features, things become more complicated because of the more complicated probe–sample interactions. Our conclusions will help to understand experimental results qualitatively, but quantitative interpretations need more complex theoretical models and numerical simulations.

References

[1] Pohl D W, Denk W and Lanz M 1984 *Appl. Phys. Lett.* **44** 651

[2] Betzig E, Trautman J K, Harris T D, Weiner J S and Kostelak R L 1991 *Science* **251** 1468

[3] Xu S F, Zhu X, Zhou H T, Shen Y M, Fei T, Zhang Y, Yin Y, Zhang B, Dai L, Liu X L, Hu J C, Lu P and Zhai Z H 2001 *Chin. Phys.* **10** S195

[4] Betzig E 1996 *Near-Field Optics*, In: Pohl D W, Courjon D (Eds) *NATO ASI Series E* Vol. 242 (Dordrecht: Kluwer)

[5] Hoffmann P, Dutoit B and Salathe R P 1995 *Ultramicroscopy* **61** 165

[6] Betzig E, Isaacson M and Lewis A 1987 *Appl. Phys. Lett.* **51** 2088

[7] Cline J A, Barshatzky H and Isaacson M 1991 *Ultramicroscopy* **38** 299

[8] Phillips P L, Knight J C, Mangan B J, Russell P St J, Charlton M D B and Parker G J 1999 *J. Appl. Phys.* **85** 6337

[9] McDaniel E B, Hsu J W P, Goldner L S, Tonucci R J, Shirley E L and Bryant G W 1997 *Phys. Rev.* B **55** 10878

[10] Bryant G W, Shirley E L, Goldner L S, McDaniel E B, Hsu J W P and Tonucci R J 1998 *Phys. Rev.* B **58** 2131

[11] Poweleit C D, Naghski D H, Lindsay S M, Boyd J T and Jackson H E 1996 *Appl. Phys. Lett.* **69** 3471

[12] Hohng S C, Yoon Y C, Kim D S, Malyarchuk V, Müller R, Lienau C, Park J W, Yoo K H, Kim J, Ryu H Y and Park Q H 2002 *Appl. Phys. Lett.* **81** 3239

[13] Hecht B, Bielefeldt H, Inouye Y, Pohl D W and Novotny L 1997 *J. Appl. Phys.* **81** 2492

[14] Campillo A L, Hsu J W P and Bryant G W 2002 *Opt. Lett.* **27** 415

[15] Born M and Wolf E 1959 *Principles of Optics* (London: Pergamon)